

DESIGNING LOW-THRUST ENABLED TRAJECTORIES FOR A HELIOPHYSICS SMALLSAT MISSION TO SUN-EARTH L5

Ian Elliott*, Christopher Sullivan Jr.*, Natasha Bosanac[†],
Farah Alibay[‡], and Jeffrey Stuart[§]

A small satellite deployed to Sun-Earth L5 could serve as a low-cost platform to observe solar phenomena such as coronal mass ejections. However, the small satellite platform introduces significant challenges in the trajectory design process via limited thrusting capabilities, power and operational constraints, and fixed deployment conditions. To address these challenges, a strategy employing dynamical systems theory is used to design a low-thrust-enabled trajectory for a small satellite to reach the Sun-Earth L5 region. This procedure is demonstrated for a small satellite that launches as a secondary payload with a larger spacecraft destined for a Sun-Earth L2 halo orbit.

INTRODUCTION

Innovative trajectory design strategies have the potential to enable small satellites to travel beyond the vicinity of Earth to observe a variety of solar processes. One possible destination for a SmallSat heliophysics mission is the Sun-Earth (SE) L5 equilibrium point, which is located at the vertex of an equilateral triangle formed with the Sun and the Earth. A spacecraft at this location offers, for instance, a perspective of the three-dimensional structure of coronal mass ejections off the Sun-Earth line while also providing a few days of advance warning of a solar storm. The Solar TERrestrial RELations Observatory B (STEREO-B) spacecraft, possessing a traditionally large form factor, drifted through the SE L5 region but did not maintain long-term bounded motion.¹ However, with the increasing availability of rideshare opportunities, small satellites may potentially be deployed to this destination within the Sun-Earth system to complete targeted, short-term science missions.

While small satellites have emerged as a low-cost option for performing on-orbit science, their form factor introduces several challenges in the trajectory design process. These challenges include constrained deployment conditions due to their status as a secondary payload as well as limited operational capabilities such as available thrust, propellant mass, and power generation. A previous investigation demonstrated a preliminary connection between these spacecraft design properties and the geometry of feasible trajectories for a 14 kg CubeSat with a 0.4 mN electrospray thruster

*Graduate Research Assistant, Smead Department of Aerospace Engineering Sciences, University of Colorado Boulder, Boulder CO, 80309

[†]Assistant Professor, Colorado Center for Astrodynamics Research, Smead Department of Aerospace Engineering Sciences, University of Colorado Boulder, Boulder CO, 80309

[‡]Systems Engineer, Jet Propulsion Laboratory, California Institute of Technology, Pasadena CA, 91109

[§]Mission Design and Navigation Systems Engineer, Jet Propulsion Laboratory, California Institute of Technology, Pasadena CA, 91109

deployed from a high-energy trajectory near the Earth.² However, the small satellite form factor can encompass a variety of masses and propulsion systems. In this work, a 6U CubeSat is considered at the lower capability end of the small satellite class that maneuvers with a low-thrust electrospray engine, currently in development as a modular, commercial off-the-shelf propulsion system.³ An 180 kg ESPA-class SmallSat with a 13 mN Hall-effect thruster is considered a current high-performance extreme of the small satellite class.² The development of a trajectory design procedure that can accommodate form factors between these two extremes, the properties of low-thrust propulsion systems and driving constraints can enable rapid small satellite mission concept development.

To design complex, low-thrust-enabled trajectories that are feasible – subject to the constraints associated with small satellite missions – dynamical systems techniques are useful.⁴ First, the dynamics of a spacecraft within the Sun-Earth system are approximated using the autonomous and conservative Circular Restricted Three-Body Problem (CR3BP). In this model, fundamental natural dynamical structures exist, including: equilibrium points, periodic orbits, quasi-periodic and manifolds. Analysis of these natural motions offers insight into the design of efficient low-thrust trajectories within multi-body systems. In particular, constants of motion and their associated bounds on feasible motion guide the design of itineraries and heuristic thrusting strategies. Furthermore, arcs along natural structures are assembled and connected via low-thrust segments to form a reasonable initial guess for an end-to-end trajectory. In the Sun-Earth system, these structures tend to reflect the geometry of motions that exist in high fidelity ephemeris models. To effectively transition a discontinuous initial guess assembled in the CR3BP to a point mass ephemeris model of the Sun-Earth-Moon system, a multiple shooting corrections strategy is used. This general procedure is outlined, improving upon previous work by Bosanac, Alibay and Stuart.² This approach is then applied to the design of a low-thrust trajectory for a SmallSat to Sun-Earth L5, demonstrating that dynamical systems theory enables the informed design of low-thrust-enabled trajectories with limited required propulsive effort as well as the incorporation of a variety of mission constraints.

DYNAMICAL MODELS

Models of increasing fidelity are leveraged within the trajectory design process with the goal of constructing a rapid and informed framework for designing complex paths subject to a variety of constraints. The use of the lower-fidelity CR3BP guides the trajectory design process via analysis and assembly of natural dynamical structures. These solutions are then combined with low-thrust segments and transitioned to a higher-fidelity point mass ephemeris model to ensure accurate modeling. This approach of gradually increasing the model fidelity reduces the computational complexity and effort required to identify feasible transfers during mission concept development.

Circular Restricted Three-Body Problem

In the Sun-Earth system, the Circular Restricted Three-Body Problem offers a representative approximation of multi-body gravitational environment. To reflect the dynamics of an assumed massless particle, P_3 , the CR3BP approximates the motion of two primary bodies – the Sun, P_1 and the Earth, P_2 – via circular orbits about the system’s mutual barycenter.⁵ The Sun-Earth rotating frame, $\hat{x}\hat{y}\hat{z}$, is defined with the origin at the system barycenter and rotates with the primary bodies, which appear fixed along the horizontal \hat{x} axis. The \hat{z} axis is defined in the direction of the angular velocity of the system, while the \hat{y} axis completes the righthanded coordinates system. This rotating frame is displayed in Figure 1 relative to the $\hat{X}\hat{Y}\hat{Z}$ inertial frame. Following nondimensionalization

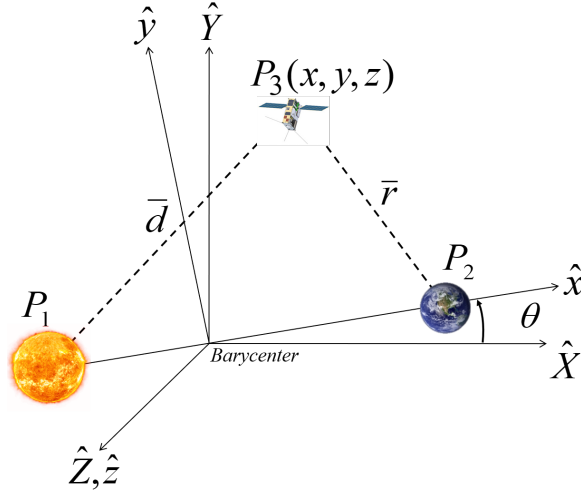


Figure 1. Description of the CR3BP with the inertial and rotating frame.

of mass, time and length quantities, the system mass ratio μ is defined as the ratio $\mu = m_2/(m_1 + m_2)$ where m_1 and m_2 are the masses of the primary bodies and $m_2 \leq m_1$. For the Sun-Earth system, the mass ratio is approximately $\mu = 3.0035 \times 10^{-6}$. Then, the nondimensional state vector $\vec{x} = [x, y, z, \dot{x}, \dot{y}, \dot{z}]^T$ is defined relative to the system's barycenter in the rotating frame. Using these definitions, the nondimensional equations of motion in the rotating frame are then written as:

$$\begin{aligned}\ddot{x} &= 2\dot{y} + x - \frac{(1-\mu)(x+\mu)}{d^3} - \frac{\mu(x-1+\mu)}{r^3} \\ \ddot{y} &= -2\dot{x} + y - \frac{(1-\mu)y}{d^3} - \frac{\mu y}{r^3} \\ \ddot{z} &= -\frac{(1-\mu)z}{d^3} - \frac{\mu z}{r^3}\end{aligned}\quad (1)$$

where $d = \sqrt{(x+\mu)^2 + y^2 + z^2}$ and $r = \sqrt{(x-1+\mu)^2 + y^2 + z^2}$. Within this model, five equilibrium points exist that are fixed in the rotating frame for a given mass ratio. The five equilibrium points can be categorized into two families: collinear equilibrium points (L1, L2, L3) and triangular equilibrium points (L4, L5).

Since the CR3BP is autonomous an integral of motion exists in the rotating frame. In fact, the Jacobi constant C_J is a energy-like constant for natural trajectories in the CR3BP, defined as

$$C_J = 2U^* - (\dot{x}^2 + \dot{y}^2 + \dot{z}^2) \quad (2)$$

where U^* is a pseudo-potential term defined as

$$U^* = \frac{1}{2}(x^2 + y^2) + \frac{1-\mu}{d} + \frac{\mu}{r} \quad (3)$$

As the Jacobi constant decreases, it is analogous to the “energy” of the natural trajectory increasing. Jacobi constant is useful for several analyses of motion in the CR3BP. The term is used to compute the theoretically reachable regions of space for a natural trajectory in the Restricted Problem and consequently, the unreachable regions of space, called forbidden regions. The boundary between the

reachable and forbidden regions of space are known as zero-velocity surfaces, and are well known in the xy plane as zero-velocity curves (ZVCs). The Jacobi constant corresponding to each of the five equilibrium points are useful for determining feasible motion for natural trajectories, namely through analysis of motion passing near L1 and L2. As the Jacobi constant of a natural trajectory decreases past the Jacobi constant of L1 and L2, the ZVCs form “gateways” around the equilibrium points. For motion in the region of the secondary body to leave the body’s vicinity, the motion must pass through either the L1 or L2 gateway. Figure 2 illustrates the ZVCS for an Jacobi constant lower than that of both L1 and L2 such that both gateways can allow motion to access the Earth vicinity. These ZVCs are displayed in a Sun-Earth rotating frame with gray shaded regions corresponding to regions of forbidden regions where a spacecraft cannot be located for a given value of the Jacobi constant. The equilibrium points are displayed as red diamonds.

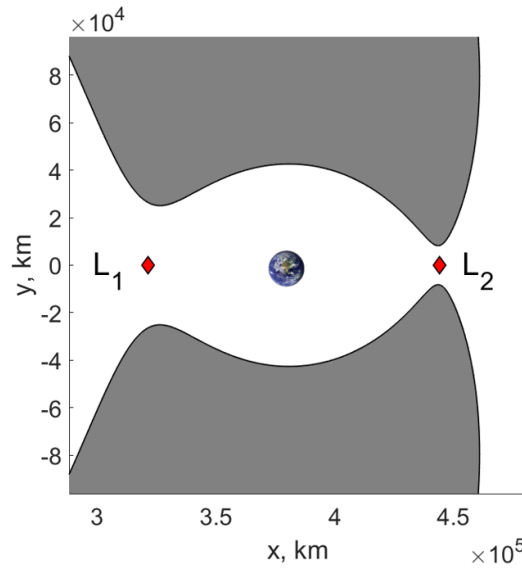


Figure 2. Zero velocity curves in the Sun-Earth system for a Jacobi constant of $C_J < C_J(L_2) < C_J(L_1)$

Spacecraft Models

Before a low-thrust trajectory can be developed, the the spacecraft’s engine performance must be defined. In order to capture the abilities of the range of the small satellite family, two spacecraft models were defined based on current technology. A 6U CubeSat model is used to represent the lower-performance end, with lower available thrust and lower specific impulse I_{sp} , of low-thrust enabled small satellites. An ESPA-class SmallSat represents small satellites with higher available thrust and I_{sp} . Table 1 is an overview of both spacecraft models referenced in this study.²

Ephemeris Model

To model the motion of a spacecraft, a point-mass ephemeris system, using information on planetary bodies and the Moon from the NASA SPICE Toolkit is used.⁸ The forces considered to act on the spacecraft are the gravitational effects of the Sun, Earth and Moon as well as a force from the low-thrust engine, \vec{F}_{lt} . The mass of the spacecraft is considered to have a negligible gravitational effect on the primary bodies. For a spacecraft with a state vector of $\vec{X} = [X, Y, Z, \dot{X}, \dot{Y}, \dot{Z}]^T$

Table 1. Baseline spacecraft configurations.

Parameter	6U CubeSat ⁶	ESPA SmallSat ⁷
Available Thrust (mN)	0.4	13
I_{sp} (s)	1250	1375
Wet Mass (kg)	14	180
Available Prop. Power (W)	10	200

defined in a Earth-centered inertial frame, the equations of motion are

$$\ddot{\vec{R}}_{E,sc} = G \left[-m_E \left(\frac{\vec{R}_{E,sc}}{R_{E,sc}^3} \right) + m_S \left(\frac{\vec{R}_{sc,S}}{R_{sc,S}^3} - \frac{\vec{R}_{E,S}}{R_{E,S}^3} \right) + m_M \left(\frac{\vec{R}_{sc,M}}{R_{sc,M}^3} - \frac{\vec{R}_{E,M}}{R_{E,M}^3} \right) \right] + \frac{\vec{F}_{lt}}{m_{sc}} \quad (4)$$

where $\vec{R} = [X, Y, Z]^T$ and the subscript sc indicates the spacecraft, E the Earth, S the Sun, and M the Moon.⁹ Other external perturbations, such as solar radiation pressure and J_2 , are not currently considered. However, the corrections process discussed in the following section allows for the future incorporation of these effects. The spacecraft's mass loss due to propellant usage is calculated using the mass flow rate equation

$$\dot{m}_{sc} = -\frac{F_{lt}}{I_{sp} g_0} \quad (5)$$

where g_0 is the gravitational acceleration measured at the surface of the Earth, $g_0 = 9.81$ m/s.

DYNAMICAL SYSTEMS THEORY

Fundamental Structures

Several structures exist in the rotating frame of the CR3BP, including: equilibrium points, periodic orbit families, and invariant manifolds. Insight into these dynamical structures is used in the trajectory design to guide trajectory construction in the chaotic regime of the Sun-Earth system.¹⁰

In a Sun-Earth CR3BP, five Lagrange points exist in the rotating frame. These locations are defined such that a spacecraft placed at these points possesses no velocity or acceleration in the rotating frame. Three of these points, the L1, L2, and L3 points are inherently unstable points meaning perturbations at these points will lead to a spacecraft quickly leaving the regions while the L4 and L5 points are stable points where motion tends to remain naturally bounded. Furthermore, these points are approximately retained in an ephemeris model whereby objects placed at these points exist have stable motion for long periods of time as seen naturally in the Trojan and Greek asteroid families that exist in the L4 and L5 regions of the Sun-Jupiter system. These points are useful to mission designers because they provide useful regions where spacecraft can be positioned to perform science with only small fuel corrections necessary in order to maintain the nominal trajectory even in the ephemeris model. However, in addition to the stability properties at these points, a number of stable motions exist within the vicinity of these points, namely periodic and quasi-periodic orbits.

Periodic orbit families exist within the CR3BP and many of them emanate from equilibrium points. Specifically focusing on periodic orbits within the vicinities of the equilibrium points, these orbits are necessary to not only construct the science orbit but also to find the natural transfers within the system. Because of their inherent instability, a number of L1, L2, and L3 periodic

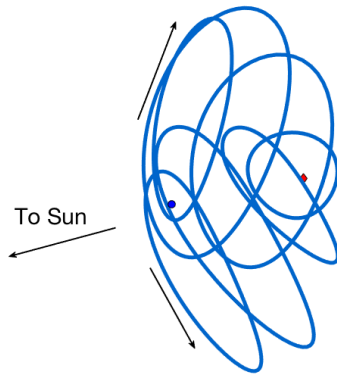


Figure 3. Sun-Earth L2 halo orbit family.

orbit families possess natural transfers, known as invariant manifolds that model the flow of natural motion to and away from these periodic orbits. Specifically taking advantage of the natural flow away from these orbits enables trajectories to conserve fuel while still traveling towards a region of interest. In contrast, the L4 and L5 periodic orbit families contain stable orbits useful for performing science for long periods of time that are approximately retained in the ephemeris model. For many members of the Lyapunov, halo, and vertical periodic orbit families near L1, L2, and L3, there exist four manifolds that exhibit the flow of natural motion: two stable, two unstable.¹¹ The two stable manifolds naturally flow onto the periodic orbit in infinite time while the two unstable manifolds guide motion away from the periodic orbit in infinite time. Examining the unstable manifolds emanating from the L2 periodic orbit families reveals that motion along a manifold trajectory will naturally travel towards the vicinity of L5. Similarly, motion that departs along an unstable manifold of an L1 orbit naturally approaches the L4 region. A natural transfer arc that connects the Earth vicinity to SE L5 can be constructed by selecting a trajectory from the unstable manifold, allowing the spacecraft to travel from the L2 gateway towards L5.

Poincaré Mapping

One method of making an informed selection of the transfer arc to use for the initial guess involves Poincaré maps.¹² This strategy involves capturing the intersection of many trajectories, such as deployment, transfer, and insertion arcs, with a hyperplane chosen by the mission designer. Representation of these intersections on a map supports selection of arcs with favorable characteristics to be utilized for the trajectory. For instance, selecting intersections of arcs with small discontinuities in the position and velocity states ensures that a corrections algorithm can correct the arcs into a single, smooth trajectory. Furthermore, TOF and CJ quantities are considered when selecting arcs so that no unnecessary time or propellant mass is needed for the final trajectory.

Corrections

In order to develop a continuous trajectory in an ephemeris model, a direct multiple shooting corrections algorithm is employed.¹³ The multiple shooting algorithm discretizes the trajectory into multiple nodes along the initial guess separated by an appropriate time step. By correcting for continuity between several nodes instead of attempting to correct a trajectory in one segment, the sensitivity of the problem is reduced. Multiple shooting additionally allows for connecting natural coasting arcs and low-thrust segments when correcting for continuity. Another critical constraint

implemented in the corrections process is the ability to fix the initial state and epoch of the trajectory. This constraint is especially important in cases of flyby events as the dynamics and structure of the trajectory are extremely sensitive. An illustrative representation of the multiple shooting corrections process is shown in Figure 4 where coasting arcs are shown in blue and low-thrust arcs are shown in red. While multiple shooting corrections does not optimize for a specific parameters, it is a powerful

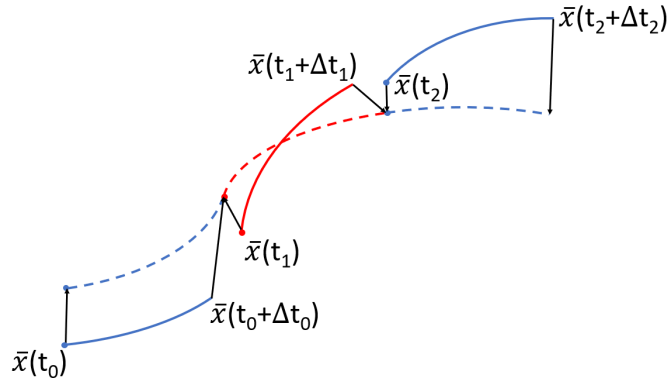


Figure 4. Illustration of the multiple shooting correction process with natural and low-thrust segments.

tool for finding continuous trajectories in an ephemeris or higher-fidelity model that retains the general structure of the initial guess.

TRAJECTORY DESIGN PROCESS

Overview

To design a low-thrust-enabled transfer from the prescribed deployment condition to the SE L5 region, the general itinerary is discretized into segments:

1. A low-thrust-enabled departure phase from deployment in Earth vicinity to the transfer through the SE L2 gateway
2. A predominantly natural transfer segment between SE L2 and SE L5
3. A low-thrust-enabled insertion into a bounded science orbit around SE L5.

This procedure is summarized graphically in Figure 5. Using the constrained deployment condition, small low-thrust maneuvers are used to explore the design space of solutions that depart through the L2 gateway. Then, natural unstable manifold structures associated with SE L2 halo orbits are analyzed to identify suitable initial guesses for the transfer segment between SE L2 and SE L5. Short period orbits that exist near L5 in the Sun-Earth CR3BP are leveraged to identify bounded motions for the science phase of the mission. After selecting a science orbit, low-thrust approach arcs are generated and analyzed for their potential to connect to the natural SE L2 orbit manifold trajectories. Poincaré mapping strategies are then used to identify arcs that reduce the discontinuities between neighboring segments. The arcs in each mission segment are assembled and connected with additional low-thrust segments to recover a feasible and efficient end-to-end trajectory in a high-fidelity ephemeris model for a SmallSat. The procedure of selecting useful arcs in each of these segments is outlined here.

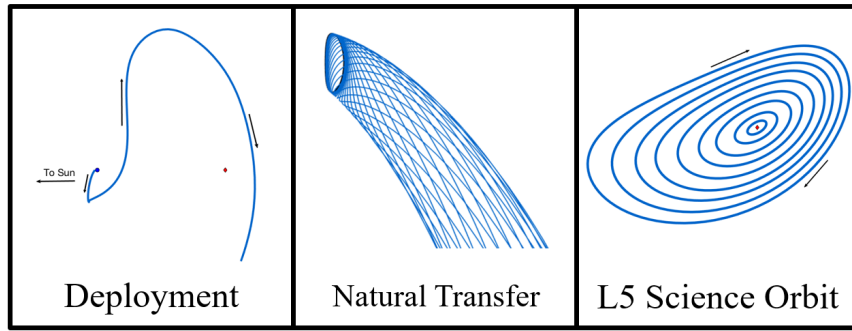


Figure 5. Illustrative representation of the trajectory design process.

Deployment and Earth Departure

The trajectory assumes a similar profile to a secondary payload deployed from a condition similar to Exploration Mission-1 (EM-1) with an epoch of October 16, 2020. Naturally propagated, the lunar flyby altitude is approximately 1698 km. Post-lunar flyby, the deployment trajectory has a Jacobi constant of approximately 3.0004. Since the Jacobi constant is lower than that of L2, both the L1 and L2 gateways are open using insight from the CR3BP. However, the Jacobi constant is still above that of L5 which implies that the trajectory has enough energy to depart through the L2 gateway towards the vicinity of L5, but not enough to reach a periodic orbit about L5.

In order to take advantage of the extreme sensitivity caused by the lunar flyby, small low-thrust maneuvers were placed before and after the flyby for both the CubeSat and SmallSat examples. A velocity, normal, co-normal (VNC) frame relative to the Earth inertial frame is used to define maneuver directions. For the SmallSat form factor, a single low-thrust anti-velocity direction maneuver

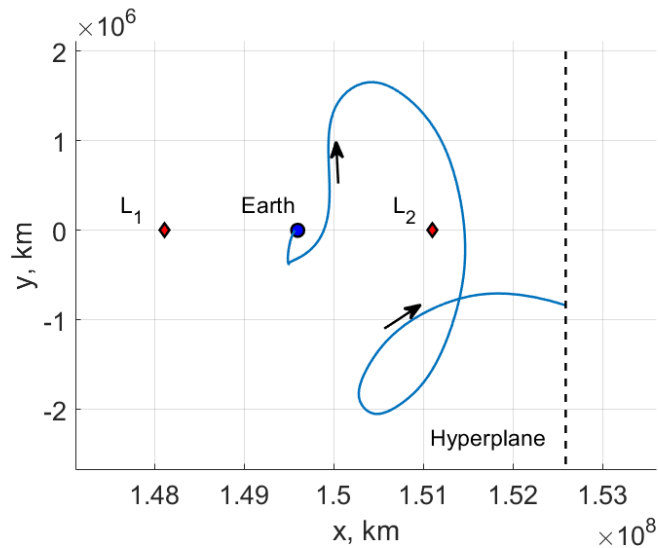


Figure 6. Sample deployment trajectory for a SmallSat from the initial conditions with a low-thrust arc prior to the lunar flyby to direct the flow of the trajectory through the SE L2 gateway without requiring significant change in Jacobi constant.

is placed after a 24 hour coast from the initial deployment. The time of flight of the maneuver is varied slightly to generate a Poincaré map and explore the possible flow of motion exiting the Earth’s vicinity via the L2 gateway. Figure 6 displays in the Sun–Earth rotating frame a sample deployment trajectory to the Poincaré map hyperplane, shown with natural coast arcs in blue and low-thrust arcs in red.

The exploration of L2 gateway departure motion through Poincaré maps was repeated for the CubeSat form factor. To account for the CubeSat’s lower control authority, two maneuvers are placed prior to the lunar flyby instead of the single maneuver in the SmallSat case. A 30 minutes anti-velocity maneuver is placed after a 24 hour coast from the initial deployment. A second maneuver, two hours in duration, is placed with a separation of ten hours from the initial maneuver. The maneuver’s thrust direction in the VNC frame is altered to create a map of possible trajectories that flow through the L2 gateway, shown in Figure 7. Nondimensional positions in the \hat{y} and \hat{z} directions are represented on the horizontal and vertical axes respectively. The velocities of the crossings \dot{y} and \dot{z} are represented with blue arrows again on the horizontal and vertical axes respectively. Finally, the marker’s color corresponds to the SE system Jacobi constant of each crossing trajectory.

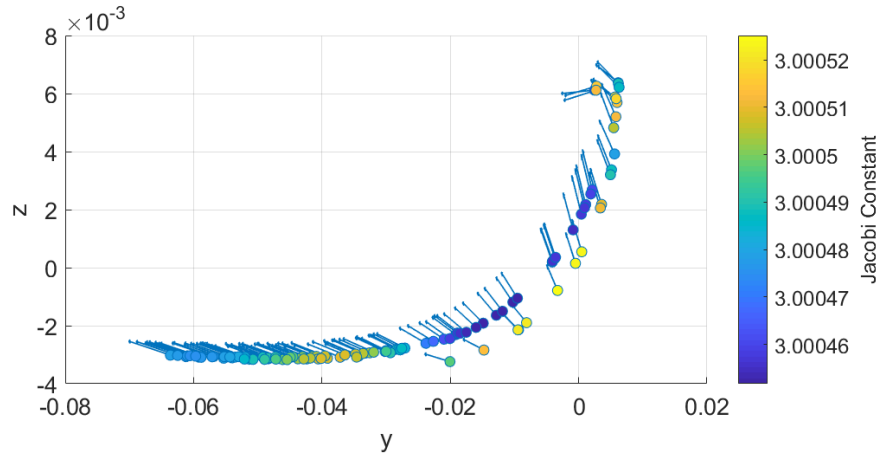


Figure 7. Poincaré map for a hyperplane near the L2 gateway for a sample of possible CubeSat departures.

Transfer From L2 to L5

To construct the transfer arc from the L2 gateway to the insertion arc into the L5 science orbit, a manifold from an L2 periodic orbit family was used since they were found to have natural motion towards L5. There are numerous L2 periodic orbit families that possess manifolds that travel towards the L5 vicinity including the SE L2 Lyapunovs, halos, axials, and vertical periodic orbit families. The L2 halo family was ultimately selected however, because they possessed similar out-of-plane components to the deployment, equivalent CJ values, and were found to have the fastest natural time of flight to L5. The L2 halo manifolds were found to have large TOF differences depending on the transfer arc chosen even though the trajectories did possess similar geometries. For instance, Figure 8 showcases an example L2 halo manifold with the fastest and slowest TOF transfers highlighted in green and red respectively.

In order to select the actual transfer arc, Poincaré maps were used to select a transfer arc with small discontinuities between both the deployment arc and insertion arc. Furthermore, a fast TOF

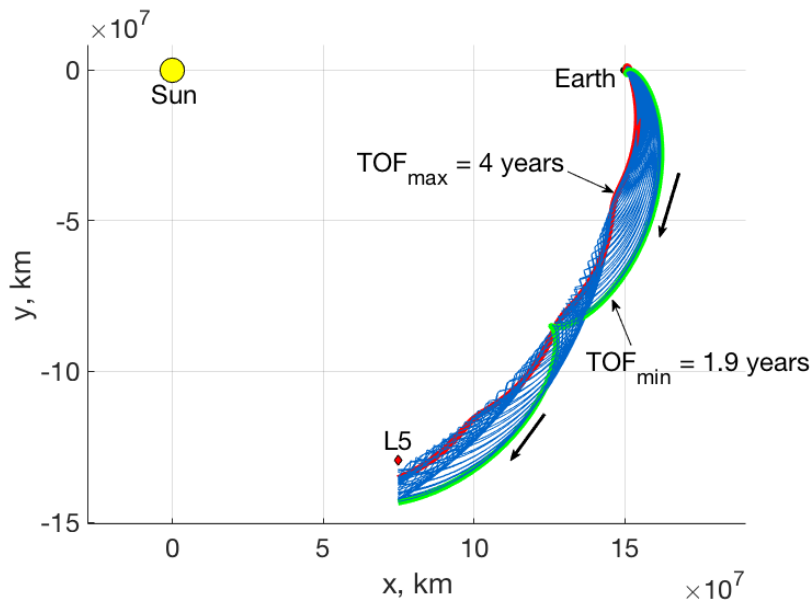


Figure 8. Sample L2 Halo orbit manifold highlighting the natural flow of motion from the vicinity of Earth to L5.

was also desirable when choosing the transfer arc so as to enable science to be performed. Fortunately, the fast TOF transfer was found to intersect close to the deployment arc while also intersecting a number of insertion arcs with a similar position, velocity, and CJ value.

Insertion into L5 Science Orbit

In order to find and select the insertion arc that will be utilized in the trajectory, first the science orbit must be chosen that accomplishes the science goals while also allowing the spacecraft to enter it with the limited fuel and thrusting constraints. A number of L5 periodic orbit families were examined including the L5 short period, long period, and vertical families. The L5 short period family was selected due to these orbits successfully accomplishing the scientific goals. However, because the energy required to get into an L5 orbit is higher than that of deployment, a low-thrust arc must be added to insert into an orbit.

An L5 science orbit with a small amplitude and lower energy was chosen as the final orbit since it required a smaller energy change than larger orbits while still satisfying the scientific constraints. To find the most favorable region of the orbit to insert into with the necessary thrust direction, the orbit was discretized into 100 nodes which were then propagated backwards for 64 different thrust profiles. The spacecraft was allowed to thrust for 1 year before switching to a natural trajectory which were propagated until the trajectories intersected a chosen hyperplane. If the resulting trajectories were found to intersect the hyperplane near the L2 manifold trajectories, they were saved and considered as viable insertion arcs. An example of a viable insertion arc intersecting the manifold transfer arcs can be seen in Figure 9.

Once all of the possible insertion arcs were found, a Poincaré map was utilized to find the most desirable insertion arc. The insertion arc with the smallest discontinuity, difference in CJ, and TOF was selected to form the basis of the initial guess as seen in Figure 10 whereby the black circle indicates the intersection of the transfer arc and insertion arc that were ultimately chosen. It can be

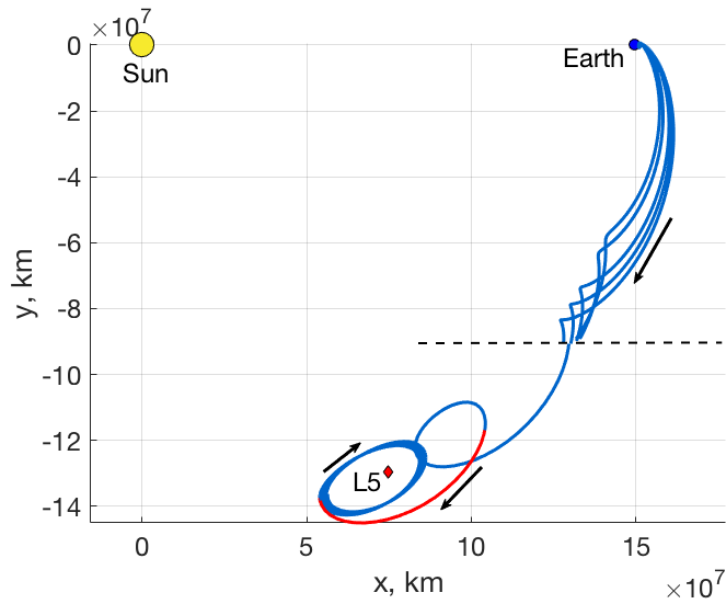


Figure 9. Insertion arc intersecting the hyperplane near possible transfer arcs.

seen that there were many viable insertion arcs to select with small discontinuities but by using a Poincaré map, deeper insights into the energy and TOF characteristics could be used to have a more informed trajectory with desirable characteristics.

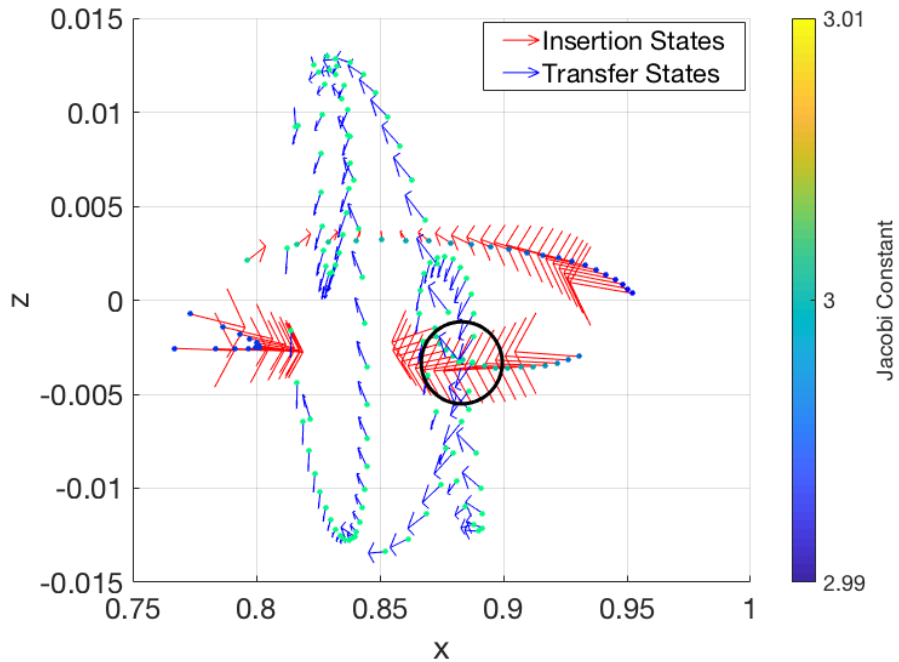


Figure 10. Poincaré map with transfer and insertion arcs highlighting the most favorable intersection.

END-TO-END TRAJECTORY POINT SOLUTIONS

After an initial guess for each segment has been selected, the deployment, transfer, and insertion segments are combined for correction in a multiple shooting algorithm. In addition to the three main segments, several revolutions of the L5 short-period science orbit are appended to the initial guess to “anchor” the solution’s boundedness around L5 after correcting to ephemeris. The multiple shooting update equation is iterated until all the norm of all constraints are below a specified tolerance, indicating a continuous solutions in the ephemeris model. If necessary, the multiple shooting process can be separated into multiple individual corrections in order to help convergence before finally correcting a single end-to-end trajectory.

Table 2. End-to-end trajectory characteristics from initial conditions to science orbit insertion.

Characteristic	6U CubeSat	ESPA SmallSat
Time of Flight (Years)	2.93	2.71
Prop. Mass Used (kg)	1.32	30.42
Lunar Flyby Altitude (km)	1641	1643

The corrections process was conducted for both the 6U CubeSat and ESPA-class SmallSat. The end-to-end trajectories produced are shown in Figure 11 and Figure 12 for the CubeSat and Small-Sat respectively in the Sun-Earth rotating frame, integrated in the Sun-Earth-Moon point-mass ephemeris system. Table 2 is an overview of the characteristics of the end-to-end trajectories for each spacecraft model. Both trajectories had time of flights from deployment to insertion into the L5 science orbit of under three years with a significant coasting phase during which science operations can be conducted.

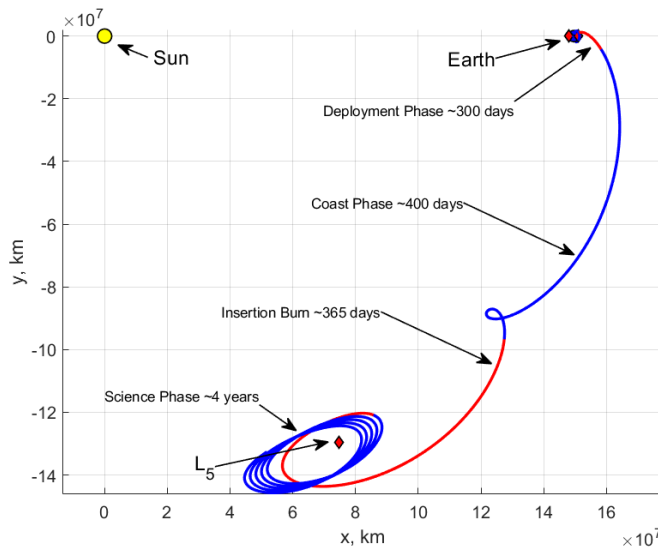


Figure 11. 6U CubeSat end-to-end trajectory from the initial conditions to a short period SE-L5 science orbit.

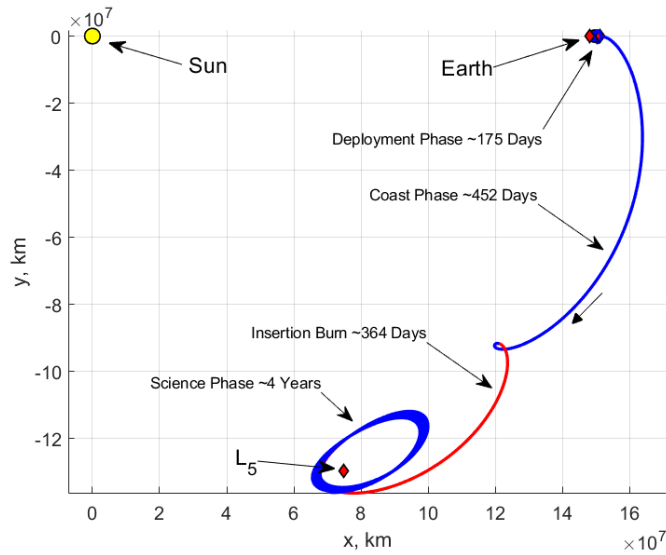


Figure 12. ESPA SmallSat end-to-end trajectory from the initial conditions to a short period SE-L5 science orbit.

Both the CubeSat and SmallSat trajectories share similar characteristics in solution geometry and time of flight. Each solution includes a revolution around L2 before departing towards L5. However, the CubeSat includes a significant low-thrust segment while passing through the L2 gateway in order to flow into the transfer phase.

CONCLUSIONS

A trajectory design process was presented to enable heliophysics missions with small satellites through a low-thrust trajectory design framework leveraging dynamical systems theory. Natural structures known to exist in the CR3BP were used as initial guess in a point-mass ephemeris system in order to efficiently develop an end-to-end trajectory. Using initial conditions similar to that of EM-1 with a high-energy lunar flyby, two example trajectories were created to a short-period science orbit around SE L5. Both a low-thrust enabled 6U CubeSat and ESPA-class SmallSat were considered to represent extreme ends of the performance range of small satellites in terms of available thrust, specific impulse, and available propellant mass. For both spacecraft models, it was found possible to insert into a bounded science orbit around L5 under three years after deployment. The trajectory design process is formulated to be flexible to different initial conditions and spacecraft parameters. Leveraging the autonomy of the CR3BP allows for trajectories to be rapidly developed as the mission parameters evolve. Future work will explore different initial conditions for rideshare opportunities for small satellites in the vicinity of Sun-Earth L2 equilibrium point.

ACKNOWLEDGEMENT

Part of this research was carried out at the Jet Propulsion Laboratory, California Institute of Technology, under a contract with the National Aeronautics and Space Administration and funded

through the Internal Strategic University Research Partnerships (SURP) program. Part of this research was also performed at the University of Colorado Boulder.

REFERENCES

- [1] M. Kaiser, T. Kucera, J. Davila, O. S. Cyr, M. Guhathakurta, and E. Christian, "The STEREO Mission: An Introduction," *Space Science Review*, 2008, pp. 5–16.
- [2] N. Bosanac, F. Alibay, and J. R. Stuart, "A Low-Thrust Enabled SmallSat Heliophysics Mission to Sun-Earth L5," *IEEE Aerospace Conference*, 2018.
- [3] D. Spence, E. Ehrbar, N. Rosenblad, N. Demmons, T. Roy, S. Hoffman, D. Williams, and V. Hruby, "Electrospray Propulsion Systems for Small Satellites," *27th Annual Conference on Small Satellites*, 2013.
- [4] N. Bosanac, A. Cox, K. Howell, and D. C. Folta, "Trajectory Design for a Cislunar CubeSat Leveraging Dynamical Systems Techniques: The Lunar IceCube mission," *27th AAS/AIAA Space Flight Mechanics Meeting in San Antonio, Texas*, 2017.
- [5] V. Szebehely, *Theory of Orbits: The Restricted Problem of Three Bodies*. London, UK: Academic Press, 1967.
- [6] A. Systems, "TILE - Tiled Ionic Liquid Electrospray," <http://www.accion-systems.com/tile>, Online; accessed October 9th 2017.
- [7] Busek, "BHT-200 Busek Hall Effect Thruster," Online; accessed October 9th 2017.
- [8] C. H. Anton, "Ancillary Data Services of NASA's Navigation and Ancillary Information Facility," *Planetary and Space Science*, No. 1, 1996, pp. 65–70.
- [9] N. Bosanac, "Leveraging Natural Dynamical Structures to Explore Multi-Body Systems, PhD Dissertation, Purdue University," 2016.
- [10] J. E. M. S. D. R. W. S. Koon, M. W. Lo, *Dynamical Systems, the Three Body Problem and Space Mission Design*. Marsden Books, 2011.
- [11] M. Lo, "Libration Point Trajectory Design," *Numerical Algorithms*, Vol. 14, 1997, pp. 153–164.
- [12] A. Haapala, *Trajectory Design in the Spatial Circular Restricted Three-Body Problem Exploiting Higher-Dimensional Poincare Maps*. PhD thesis, Purdue University, 2014.
- [13] T.A.Pavlak, *Trajectory Design and Orbit Maintenance Strategies in Multi-Body Dynamical Regimes*. PhD thesis, Purdue University, 2013.